THE ASTROPHYSICAL JOURNAL, 318:794–808, 1987 July 15

THRESHOLDS FOR RAPID MASS TRANSFER IN BINARY SYSTEMS. I. POLYTROPIC MODELS

MICHAEL S. HJELLMING AND RONALD F. WEBBINK
Department of Astronomy, University of Illinois
Received 1986 September 15; accepted 1986 December 22

ABSTRACT

The stability of a lobe-filling star in close binary systems against mass loss on a dynamical time scale is determined by the adiabatic response of that star to mass loss. The adiabatic properties (radii as functions of remnant mass) of three families of polytropic models are explored here: (1) complete polytropes, of polytropic degree n ($3/2 \leq n \leq 4$) and adiabatic index γ ($1.4 \leq \gamma \leq 2.0$) throughout; (2) composite polytropes, consisting of $n_c = 3$, $\gamma_c = 5/3$ cores with $n_e = 3/2$, $\gamma_e = 5/3$ envelopes; and (3) condensed polytropes, consisting of $n = 3/2$, $\gamma = 5/3$ envelopes with core point masses of mass fraction m_c ($0 \leq m_c \leq 1$). Mass loss is parameterized by a variation of the central pressure, the result of which is calculated by a reformulation of the Lane-Emden equation in Lagrangian (mass) coordinates.

For conservative mass transfer, models with insentropic envelopes are linearly unstable to dynamical time scale mass loss if the initial mass ratio (donor/accretor) exceeds a finite limit, q_0. For a complete polytrope with $n = 3/2$ and $\gamma = 5/3$, $q_0 = 0.634$. Models with radiative envelopes are linearly stable for any finite mass ratio ($q_0 \rightarrow \infty$), but are subject to a finite-amplitude instability (a transition from thermal to dynamical time scale mass transfer) if the initial mass ratio exceeds a critical value, q_1. For a complete polytrope with $n = 3$ and $\gamma = 5/3$, $q_1 = 2.14$. Composite polytropes are of intermediate stability, with q_0 and q_1 decreasing monotonically to the isentropic limit, $q_0 = q_1 = 0.634$, as the envelope mass fraction increases to unity. Condensed polytropes expand in response to mass loss for small fractional core masses, $m_c < 0.214$, and become stable against dynamical time scale mass transfer (at unit mass ratio) for large fractional core masses, $m_c > 0.458$. The limitations of these models, and their relevance to binary evolution (particularly common envelope evolution) are discussed.

Subject headings: stars: binaries — stars: mass loss

I. INTRODUCTION

A unique feature of binary evolution is the process of mass transfer. Many examples of unusual phenomena are known to be the result of mass transfer in binaries: Algol binaries, contact binaries, and cataclysmic variables, to name a few. Each of these examples is at present in a slow phase of mass transfer, thus accounting for their relatively high frequencies of occurrence among interacting binary stars. The evolution of systems which transfer mass on more rapid time scales differs not only in the lifetime of their interactive state, but qualitatively in the course of their evolution as well. At mass transfer rates comparable with the thermal rate for the donor star (its mass divided by its thermal relaxation, or Kelvin-Helmholtz, time scale), the accreting star is forced far from thermal equilibrium, tending to evolve into contact in Algol-type binaries (Benson 1970; Yungel'son 1973; and many others), or to a shell-burning giant-like stage in cataclysmic systems (Paczyński and Żytkow 1978; Iben 1982; Fujimoto 1982*a*, *b*). Still more rapid transfer, on time scales comparable with the orbital period (dynamical time scale) of the binary, probably lead to complete engulfment of the accreting star, creating a common envelope binary (Paczyński 1976). The evolution of these objects is almost certainly characterized by the loss of much of the initial mass of the binary, and most of its initial angular momentum. If the binary survives, this process may lead to the formation of cataclysmic binaries (Meyer and Meyer-Hofmeister 1979) or other compact, highly evolved systems. Thus the evolution of different types of close binary systems to their observed state, and indeed their stability in that state, depends fundamentally on how the donor star reacts to mass loss.

A star responds to mass loss on two time scales. The immediate response is adiabatic—hydrostatic equilibrium is restored (except for the immediate region surrounding the inner Lagrangian point), but negligible heat transport occurs on this dynamical time scale. Over a longer period of time the star regains thermal equilibrium by redistributing its internal energy to account for its new distribution of energy sources and mass.

The actual time scale for mass transfer is set by comparing these two responses to the change in the dimension of a star's Roche lobe due to the changing mass ratio (see, e.g., Webbink 1985). We can describe the result of mass loss with the radius-mass exponents, $\zeta \equiv d \ln R/d \ln M$, corresponding to the response of the Roche lobe itself (ζ_L), the adiabatic hydrostatic stellar response (ζ_{ad}), or the thermal-equilibrium stellar response (ζ_{th}). If $\zeta_L > \zeta_{ad}$, the star cannot remain within its Roche lobe in hydrostatic equilibrium, and mass transfer occurs on a dynamical time scale: the actual mass-loss rate is only limited by the sonic flow of gas through the inner Lagrangian point. If $\zeta_{ad} > \zeta_L > \zeta_{th}$, the star may remain within its Roche lobe in hydrostatic, but not thermal, equilibrium: relaxation toward thermal equilibrium requires a radius greater than R_L, driving mass transfer on the thermal time scale of the donor star. If $(\zeta_{ad}, \zeta_{th}) > \zeta_L$, mass transfer occurs only by virtue of the slow expansion of the star due to nuclear evolution, or of the contraction of its Roche lobe caused by the loss of angular momentum by gravitational radiation or mag-

netic stellar winds. (In the case where $\zeta_{th} > \zeta_{ad} > \zeta_L$, the mass-loss rate rises briefly to a thermal time scale rate until a state of thermal disequilibrium is established, whereupon the mass-loss rate subsides to the longer time scale; see Rappaport, Joss, and Webbink 1982.)

In most studies of binary evolution to date, the stability of a binary at the onset of mass transfer, whether against thermal or dynamical time scale mass transfer, has sufficed to set the pattern for its entire subsequent evolution. Qualitatively, one finds that stars with radiative envelopes are unstable to thermal time scale mass loss if their masses much exceed those of their companion stars, whereas stars with deep convective envelopes are unstable to dynamical time scale mass loss if their masses exceed roughly two-thirds those of their companions (Paczyński 1965; Paczyński; Ziółkowski, and Żytkow 1969; Plavec, Ulrich, and Polidan 1973). As explained by Webbink (1985), the ability of a star with a deep radiative envelope to contract rapidly in response to mass loss is intimately connected with the steep entropy gradient in its outer envelope which is responsible for suppressing convection. Stars with flat entropy profiles, on the other hand, tend to expand in response to mass loss. It must be stressed, however, that for a given binary to be stable against thermal or dynamical time scale mass transfer, the criteria outlined above must be satisfied not only initially, but throughout the course of mass transfer.

An example of a binary which evolves, during the course of mass exchange, from a state which is stable against dynamical time scale mass transfer to an unstable one may be found in the model calculation by Webbink (1977) of the evolution of a $1.50\ M_\odot + 0.50\ M_\odot$ binary. The initial orbital separation was such that the more massive component filled its Roche lobe while still in core hydrogen burning. The specific entropy profiles of this $1.50\ M_\odot$ star at four epochs during mass transfer (see Table 1 in Webbink 1977) are shown in Figure 1. From the onset of mass transfer (epoch 1) to epoch 2, the mass-loss rate accelerates to a thermal time scale, where it remains roughly constant in time before ultimately accelerating to a dynamical time scale (epochs 3 to 4) after it had lost $0.29\ M_\odot$. One sees that, by the time the system reaches the transition to dynamical time scale mass transfer (epoch 3), the entropy maximum near the surface of the mass-losing primary has diminished to a small fraction of its initial magnitude—the stellar envelope is much nearer an isentropic state. Furthermore, the asymptotic entropy profile differs relatively little from that obtaining at the onset of mass loss. That is, even in thermal time scale mass transfer, most of the thermal evolution of the stellar interior occurs in the surface layers, where the specific internal energy of the gas is relatively small, and very little heat transport occurs in the deep interior, where the specific internal energy of the gas is large.

In this study, we will exploit the nearly isentropic evolution of the interior of a star undergoing rapid mass loss to estimate threshold conditions for the occurrence of dynamical time scale mass transfer. We freeze the entropy profile of the donor star at the instant it begins transferring mass to its binary companion. We then argue that, so long as the mass transfer rate is not slower than the thermal rate for the donor star, it cannot contract more rapidly than a sequence of models of decreasing mass sharing the same specific entropy profile. If mass transfer occurs only on a thermal time scale, some of the energy deficit of the surface layers may be restored by energy outflow from the interior (as illustrated in Fig. 1), thus allowing the star to exceed this minimum radius and continue to drive mass transfer. However, for the mass-losing star to con-

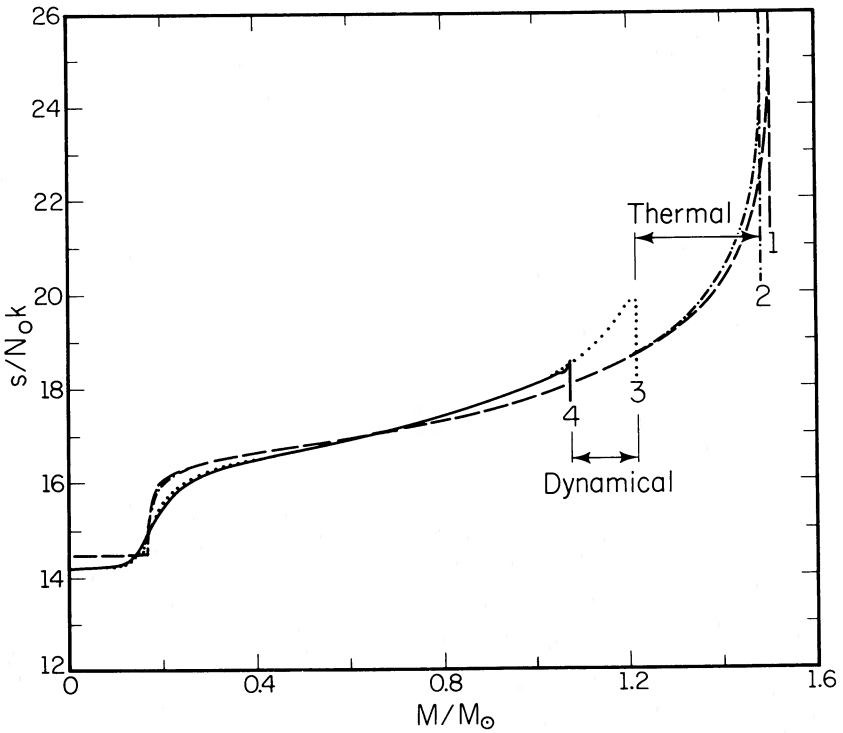

FIG. 1.—Specific entropy profiles at four epochs in the evolution of a $1.5\ M_\odot$ star undergoing rapid mass loss (Webbink 1977). Curve 1 (*dashed line*) represents the star at the onset of mass loss. From curve 2 (*dash-dotted line*) to curve 3 (*dotted line*), mass loss proceeds on a thermal time scale, then accelerates, from curve 3 to curve 4 (*solid line*), to a dynamical time scale.

tract more rapidly than the adiabatic model sequence, it would need to be capable of shedding its envelope energy excess more rapidly than on a dynamical time scale, a clear impossibility if that star is not dynamically unstable to collapse. A comparison of our adiabatic model sequences with the behavior of the Roche lobe then defines the threshold condition for dynamical time scale mass transfer.

We will explore here the properties of polytropic models for mass-losing stars. By their nature, such models omit any treatment of energy generation or heat flow, and so are not useful for investigations of stability against thermal time scale mass transfer. However, they do permit us to examine the dynamical properties of very idealized stars, hopefully to gain insight into the behavior of more realistic models. We consider here three broad types of models:

1. *Complete polytropes.* These are the classical solutions to the Lane-Emden equation, as described, for example, by Chandrasekhar (1939). They make suitable models for main-sequence stars of intermediate or low mass, but we have extended these studies to a wide range of combinations of polytropic and adiabatic indices.

2. *Composite polytropes.* Models with $n = 3/2$ envelopes fitted to $n = 3$ cores are relevant to main-sequence stars of subsolar mass, roughly 0.3 to 1.1 $M_\odot$. We consider here a series of models with different ratios of envelope mass to total mass, but with a constant adiabatic index, $\gamma = 5/3$, throughout. (Models with $n = 3/2$ cores and $n = 3$ envelopes might be suitable for upper main-sequence stars, but for the fact that the growing ratio of radiation to gas pressure renders a polytropic equation of state with constant γ unrealistic.)

3. *Condensed polytropes.* These are $n = 3/2$ envelopes fitted to point mass cores, suitable as models of red giant stars. A full range of ratios of core to total mass is explored, again under the assumption that $\gamma = 5/3$.

Sections II, III, and IV describe these polytropic calculations. Their implications for the stability of lobe-filling components in interacting binary systems are discussed in § V. Convenient transformations between the present formalism and those employed in previous studies are provided in an Appendix.

II. COMPLETE POLYTROPES

Complete polytropes can be described by the combination of the equations for hydrostatic equilibrium and mass continuity with the assumption of a power-law relation between the pressure and density, $P = K\rho^{1+1/n}$. The constant n represents the degree of the polytrope. The solutions to the resulting Lane-Emden equation are described by Chandrasekhar (1939) and tabulated by the British Association for the Advancement of Science (1932). Service (1977) has derived accurate approximations to these solutions. The conventional approach has been Eulerian, using a scaled radius as the independent variable. Under adiabatic changes, however, a star's entropy profile remains constant in the mass coordinate. In our formulation, we have therefore chosen a Lagrangian approach, with mass as the independent variable.

To simplify the Lagrangian counterpart of the Lane-Emden equation and to avoid singularities at the origin, we use a masslike variable, where $\mu = m^{1/3}$. The equations of hydrostatic equilibrium and mass continuity become, respectively,

$$\frac{dP}{d\mu} = -\frac{3G}{4\pi}\frac{\mu^5}{r^4}, \tag{1}$$

$$\frac{dr}{d\mu} = \frac{3}{4\pi}\frac{\mu^2}{\rho r^2}. \tag{2}$$

The derivative of the first equation, with a substitution of the second, becomes

$$\frac{d^2P}{d\mu^2} = \frac{5}{\mu}\frac{dP}{d\mu} + \frac{9G}{4\pi^2}\left(\frac{4\pi}{3G}\right)^{7/4}\frac{1}{\rho}\left(-\frac{1}{\mu}\frac{dP}{d\mu}\right)^{7/4}. \tag{3}$$

The variables can be made dimensionless using the polytropic equation of state, together with the scaling relations,

$$P = P_c\,\theta, \tag{4}$$

$$\mu = ax, \tag{5}$$

where P_c is the central pressure and

$$a \equiv \left(\frac{3}{\pi}\right)^{2/3}\left(\frac{4\pi}{3G}\right)^{1/2} K^{2n/3(n+1)} P_c^{(3-n)/6(n+1)}. \tag{6}$$

The Lagrangian polytropic equation then becomes

$$\frac{d^2\theta}{dx^2} = \frac{5}{x}\frac{d\theta}{dx} + \theta^{-n/(n+1)}\left(-\frac{1}{x}\frac{d\theta}{dx}\right)^{7/4}. \tag{7}$$

The boundary conditions at $x = 0$ may be found by letting $\mu^3 = 4\pi\rho r^3/3$, for small μ, and substituting into equation (1), giving

$$\theta = 1, \tag{8a}$$

$$\frac{1}{x}\frac{d\theta}{dx} = -2^{8/3}. \tag{8b}$$

The series solution to equation (7) for small x is then

$$\theta(x) = 1 - 2^{5/3}x^2 + \frac{8}{5}\frac{n}{n+1}2^{1/3}x^4 - \cdots. \tag{9}$$

The radius can be evaluated at any point by rewriting the equation of hydrostatic equilibrium:

$$r^4 = \frac{3G}{4\pi P_c}\frac{a^6x^5}{-d\theta/dx}. \tag{10}$$

For our purposes here, we define a dimensionless radius,

$$z \equiv \left(\frac{3}{\pi}\right)^{1/3}\left(\frac{x^5}{-d\theta/dx}\right)^{1/4} \tag{11}$$

such that the dimensionless central density, $3x^3/4\pi z^3$, is unity.

These relations can be extended to include adiabatic mass loss from the polytrope. A polytrope's mass and radius are determined by the values of K and P_c. In order to preserve the simplicity of classical polytropic models, in which the boundary conditions are imposed at the center, we effect changes to the mass and radius of the polytrope by varying P_c, keeping K fixed. For the purposes of this paper, we will refer to this variation of P_c as a perturbation to the structure of the polytrope, although the magnitude need not be small. In the calculation we assume hydrostatic equilibrium, which places an upper limit on the applicable transfer rate, and a constant entropy profile, which implies a lower limit beyond which thermal relaxation cannot be neglected.

Let us define a new variable to describe the effect of any perturbations,

$$\omega(x) \equiv P(x)/P_0(x) = (\rho/\rho_0)^\gamma,$$

where $\gamma \equiv (\partial \ln P/\partial \ln \rho)_s$. The new pressure, $P(x)$, satisfies the requirement of hydrostatic equilibrium if it is a solution of the Lagrangian polytropic equation. By substituting $\omega\theta$ into equation (7) and subtracting ω times equation (7), we obtain an equation which describes the change in the pressure throughout the polytrope:

$$\frac{d^2\omega}{dx^2} = \left(\frac{5}{x} - \frac{2}{\theta}\frac{d\theta}{dx}\right)\frac{d\omega}{dx} + [\omega^{1/\gamma}\theta^{(2n+1)/(n+1)}]^{-1} \times \left\{\left[-\frac{1}{x}\frac{d}{dx}(\omega\theta)\right]^{7/4} - \omega^{1+1/\gamma}\left(-\frac{1}{x}\frac{d\theta}{dx}\right)^{7/4}\right\}. \quad (12)$$

The boundary conditions at $x = 0$ may be found in the same way as above (eqs. [8a] and [8b]):

$$\omega = \omega_0 , \quad (13a)$$

$$\frac{1}{x}\frac{d\omega}{dx} = -2^{8/3}\omega_0 f , \quad (13b)$$

where $f = \omega_0^{4/(3\gamma)-1} - 1$. From these conditions and equation (12) a series solution for small x can be found:

$$\omega(x) = \omega_0\left\{1 - 2^{5/3}fx^2 + \frac{2}{5}2^{10/3} \times \left[\frac{1}{\gamma}f^2 - f\left(\frac{3}{2} - \frac{1}{\gamma} - \frac{n}{n+1}\right)\right]x^4 - \cdots\right\}. \quad (14)$$

The difference in pressure causes a change in the radius of each mass point. The new radius may be found by replacing $d\theta/dx$ with $d(\omega\theta)/dx$ in equation (10).

The mass loss is parameterized by the change in the central pressure ω_0. A loss of mass produces a decrease in the central pressure ($\omega_0 < 1$), and the interior must expand to larger radii. In the surface layers the lower pressure results in $P(x) = 0$ occurring at a smaller x. Whether there is an overall expansion or contraction depends upon the relation between these two effects. Note that for $\gamma = 4/3$, ω equal to a constant is a solution of equation (12). This also follows from the series expansion, equation (14), since $f = 0$. The result is $M = M_0$, and from equation (10), $R = \omega_0^{-1/4}R_0$—the mass of the perturbed polytrope does not change; only its radius is varied by the perturbation. This reflects the fact that $\gamma = 4/3$ configurations have zero total energy and lie at the point of marginal virial instability.

For the case $\gamma = 1 + 1/n$, the result of a change in the central pressure is a homologous transformation of the standard solution, θ, in the x-coordinate. Making the substitutions $x = cy$ and $\omega(x)\theta(x) = c^\beta\theta(y)$ in equation (3), we find that $\beta = 6(n + 1)/(3 - n)$, and $c = \omega_0^{1/\beta}$. The corresponding changes in the mass and radius are

$$M = \omega_0^{(3-n)/2(n+1)}M_0 , \quad (15)$$

$$R = \omega_0^{(1-n)/2(n+1)}R_0 , \quad (16)$$

resulting in the familiar mass-radius relation: $R/R_0 = (M/M_0)^{(1-n)/(3-n)}$. For the case of $\gamma \neq 1 + 1/n$, no such transformation exists: the final values of M and R are nontrivial functions of n, γ, and ω_0.

To solve equations (7) and (12), thus calculating the adiabatic response of mass-losing polytropes, the series solutions were used to find the first points with $\Delta x = 10^{-4}$. We chose the Adams-Bashforth-Moulton predictor-corrector scheme (Acton 1970) to continue the integration of the differential equations. This scheme requires four previous points to advance in the x-coordinate. It avoids the known instability of the Milne predictor-corrector in solving for decreasing functions. Since the problem is one-dimensional, variable storage is not a problem, and this method requires the evaluation of the differential equation only half as often as the more common Runge-Kutta method. In order to maintain well-behaved values for both R_0 and R, we decreased Δx at preselected values of θ and ω to a minimum of $\Delta x = 10^{-4}/2^{28}$.

The calculations, for a given n and γ, generally used 15 starting values of $\rho_c/\rho_{c0} = \omega_0^{1/\gamma}$ ranging from 0.999 to 0.1, providing a range of final masses: $-1.0 < \ln M/M_0 < 0.0$. The models covered a parameter space of $n \in [3/2, 2, 5/2, 3, 7/2, 4]$ and $\gamma \in [2, 7/4, 5/3, 3/2, 7/5]$, with $\gamma \geq 1 + 1/n$, thus ensuring that the entropy gradient through the star did not become negative (see eq. [17] below). Additional values of $4/3 < \gamma < 5/3$ for $n = 3$ were examined. The results are given in Table 1 with a precision of ± 3 in the last digit quoted. The first column gives the ratio of perturbed to equilibrium central densities ($= \omega_0^{1/\gamma}$), the second the dimensionless mass, the third the dimensionless radius, and the fourth the local radius-mass exponent, ζ.

We should note the physical significance of the choice of n and γ. An ideal gas has the following expression for its specific entropy:

$$s(m) = s_0 + c_v \ln (P/\rho^\gamma) = s_0 + c_v \ln K + (1 + 1/n - \gamma)c_v \ln \rho . \quad (17)$$

An isentropic gas, where $ds/dm = 0$, will have $n = 1/(\gamma - 1)$. This is also the criterion for neutral stability against convection. Perfect monatomic gases have $\gamma = 5/3$, so a convective region in a star can be described with a polytropic degree of $n = 3/2$. If $n > 1/(\gamma - 1)$, $ds/dm > 0$, and the region is stable against convection. In the idealized case where the ratio of radiation pressure to total pressure is a constant throughout a region, that region behaves like a polytropic gas of degree $n = 3$. If $n < 1/(\gamma - 1)$, $ds/dm < 0$, and the gas is convectively unstable. Even modestly efficient convection will force n near to its isentropic value, and so strongly superadiabatic structures do not occur among hydrostatic stars except at small optical depths from their surfaces. For this reason we have not pursued such models.

Figures 2 and 3 contain the adiabatic response curves of a few of the complete polytropes including the idealized fully convective ($n = 3/2$, $\gamma = 5/3$) and fully radiative ($n = 3$, $\gamma = 5/3$) models. All of the models in which $\gamma > 1 + 1/n$ contract at the beginning of mass loss. The entropy profiles of these models have a positive slope, so $s(m)$ goes asymptotically to infinity at the surface. As mass is removed, the gas now in the outer envelope has lower specific entropy, and so is denser than the initial envelope, causing the star to become more compact. However, as mass is continually removed, the entropy profile becomes flatter and the remnant core becomes nearly isentropic. Thus the contraction is ultimately replaced by an overall expansion appropriate for the particular value of γ, regardless of n. This behavior corresponds to the limit of very large perturbations.

For $\omega_0 \ll 1$, the slope of the adiabatic response approaches an asymptotic value. A very large change in the central quantities results in $\omega(x)$ going to zero while $\theta(x) \approx 1$, so that $P \approx K\rho^\gamma$, where $K^{1+1/n} = K_0^\gamma P_{c0}^{1+1/n-\gamma}$ (K_0 and P_{c0} being the unperturbed polytropic constant and central pressure, respectively). By using the standard expressions in the radial

TABLE 1

ADIABATIC RESPONSES OF MASS-LOSING COMPLETE POLYTROPES

ρ_c/ρ_{c0}	x^3	z	ζ_{ad}
Complete Polytrope: $n = 3/2$, $\gamma = 7/4$, $\chi = 0.905861$, $\eta = 0.048530$, $q_1 = 0.902$			
1.000.....	0.387122	0.821135	...
0.999.....	0.386855	0.818907	1.578
0.995.....	0.385792	0.816969	0.551
0.99	0.384466	0.815797	0.323
0.95	0.373878	0.813112	0.027
0.90	0.360575	0.813537	−0.044
0.85	0.347124	0.815464	−0.077
0.80	0.333483	0.818358	−0.098
0.75	0.319615	0.822035	−0.112
0.70	0.305484	0.826442	−0.124
0.65	0.291053	0.831588	−0.133
0.5	0.245502	0.852153	−0.152
0.4	0.212631	0.871672	−0.162
0.3	0.176832	0.898849	−0.170
0.2	0.136549	0.940328	−0.178
0.1	0.087984	1.01876	−0.184
Complete Polytrope: $n = 3/2$, $\gamma = 2$, $\chi = 0.769053$, $\eta = 0.150658$, $q_1 = 1.261$			
1.000.....	0.387122	0.821135	...
0.999.....	0.386584	0.811483	3.650
0.995.....	0.384477	0.801899	1.531
0.99	0.381895	0.795154	1.058
0.95	0.362211	0.768937	0.442
0.90	0.338947	0.751019	0.293
0.85	0.316627	0.738058	0.225
0.80	0.295014	0.727579	0.183
0.75	0.273978	0.718637	0.153
0.70	0.253436	0.710754	0.131
0.65	0.233326	0.703648	0.113
0.5	0.175203	0.685392	0.075
0.4	0.138030	0.674840	0.057
0.3	0.101962	0.665006	0.041
0.2	0.066925	0.655468	0.028
0.1	0.032900	0.645605	0.016
Complete Polytrope: $n = 2$, $\gamma = 5/3$, $\chi = 0.727645$, $\eta = 0.136598$, $q_1 = 1.134$			
1.000.....	0.452071	1.07160	...
0.999.....	0.451769	1.05781	6.878
0.995.....	0.450577	1.04732	2.470
0.99	0.449105	1.04071	1.563
0.95	0.437572	1.01974	0.445
0.90	0.423348	1.00980	0.192
0.85	0.409122	1.00534	0.079
0.80	0.394789	1.00385	0.009
0.75	0.380276	1.00447	−0.039
0.70	0.365519	1.00681	−0.076
0.65	0.350457	1.01069	−0.105
0.5	0.302761	1.03180	−0.170
0.4	0.267974	1.05559	−0.201
0.3	0.229470	1.09155	−0.229
0.2	0.184972	1.15000	−0.253
0.1	0.128673	1.2671	−0.282
Complete Polytrope: $n = 2$, $\gamma = 7/4$, $\chi = 0.672918$, $\eta = 0.184249$, $q_1 = 1.330$			
1.000.....	0.452071	1.07160	...
0.999.....	0.451646	1.05055	7.591
0.995.....	0.449989	1.03422	2.848
0.99	0.447962	1.02372	1.854
0.95	0.432428	0.988044	0.633
0.90	0.413790	0.967756	0.357
0.85	0.395558	0.955287	0.232
0.80	0.377530	0.946803	0.156
0.75	0.359587	0.940909	0.103
0.70	0.341639	0.936964	0.063
0.65	0.323615	0.934616	0.031
0.5	0.268393	0.935907	−0.038
0.4	0.229852	0.944074	−0.072
0.3	0.188923	0.960330	−0.100
0.2	0.144023	0.990585	−0.126
0.1	0.091367	1.05605	−0.150
Complete Polytrope: $n = 2$, $\gamma = 2$, $\chi = 0.589289$, $\eta = 0.284038$, $q_1 = 1.675$			
1.000.....	0.452071	1.07160	...
0.999.....	0.451178	1.02960	7.430
0.995.....	0.447817	0.997261	2.907
0.99	0.443829	0.976533	1.956
0.95	0.415330	0.905289	0.776
0.90	0.383797	0.862206	0.505
0.85	0.354811	0.833037	0.384
0.80	0.327598	0.810453	0.310
0.75	0.301755	0.791801	0.259
0.70	0.277034	0.775783	0.221
0.65	0.253266	0.761656	0.190
0.5	0.186600	0.726603	0.125
0.4	0.145321	0.707068	0.095
0.3	0.106160	0.689295	0.069
0.2	0.068911	0.672428	0.047
0.1	0.033479	0.655344	0.026
Complete Polytrope: $n = 5/2$, $\gamma = 3/2$, $\chi = 0.658291$, $\eta = 0.134403$, $q_1 = 0.794$			
1.000.....	0.516785	1.42402	...
0.999.....	0.516616	1.40309	13.77
0.995.....	0.515946	1.39022	4.377
0.99.....	0.515115	1.38285	2.556
0.95	0.508510	1.36404	0.430
0.90	0.500180	1.36041	−0.025
0.85	0.491666	1.36357	−0.224
0.80	0.482907	1.37069	−0.346
0.75	0.473849	1.38085	−0.429
0.70	0.464442	1.3937	−0.493
0.65	0.454627	1.40927	−0.545
0.5	0.422000	1.47428	−0.655
0.4	0.396513	1.53849	−0.710
0.3	0.366290	1.6308	−0.758
0.2	0.328045	1.7779	−0.806
0.1	0.272452	2.07448	−0.846
Complete Polytrope: $n = 5/2$, $\gamma = 5/3$, $\chi = 0.523688$, $\eta = 0.275250$, $q_1 = 1.586$			
1.000.....	0.516785	1.42402	...
0.999.....	0.516308	1.36510	14.55
0.995.....	0.514480	1.32726	5.166
0.99	0.512274	1.30426	3.309
0.95	0.495790	1.23099	1.098
0.90	0.476425	1.19166	0.616
0.85	0.457679	1.16804	0.404
0.80	0.439243	1.15207	0.276
0.75	0.420937	1.14091	0.187
0.70	0.402635	1.13325	0.120
0.65	0.384234	1.12840	0.066
0.5	0.327470	1.12789	−0.048
0.4	0.287247	1.13950	−0.104
0.3	0.243674	1.16407	−0.152
0.2	0.194396	1.21110	−0.196
0.1	0.133509	1.31541	−0.237
Complete Polytrope: $n = 5/2$, $\gamma = 7/4$, $\chi = 0.493017$, $\eta = 0.324230$, $q_1 = 1.792$			
1.000.....	0.516785	1.42402	...
0.999.....	0.516102	1.34694	13.49
0.995.....	0.513535	1.29793	4.889
0.99	0.510486	1.26830	3.174
0.95	0.488417	1.17414	1.117
0.90	0.463397	1.12261	0.666
0.85	0.439799	1.09042	0.468
0.80	0.417070	1.06734	0.348
0.75	0.394917	1.04980	0.264
0.70	0.373150	1.03611	0.202
0.65	0.351625	1.02535	0.152
0.5	0.287398	1.00631	0.046
0.4	0.243840	1.00333	−0.006
0.3	0.198535	1.00940	−0.050
0.2	0.149832	1.02970	−0.089
0.1	0.093929	1.08427	−0.126

TABLE 1—*Continued*

ρ_c/ρ_{c0}	x^3	z	ζ_{ad}
Complete Polytrope: $n = 5/2$, $\gamma = 2$, $\chi = 0.443454$, $\eta = 0.426483$, $q_1 = 2.154$			
1.000.....	0.516785	1.42402	...
0.999.....	0.515298	1.29761	10.47
0.995.....	0.510035	1.22116	3.950
0.99	0.504068	1.17638	2.627
0.95	0.464616	1.03911	1.017
0.90	0.423980	0.965010	0.658
0.85	0.388163	0.917622	0.498
0.80	0.355481	0.882245	0.402
0.75	0.325115	0.853797	0.336
0.70	0.296581	0.829877	0.285
0.65	0.269560	0.809146	0.246
0.5	0.195595	0.759070	0.162
0.4	0.150962	0.731936	0.122
0.3	0.109350	0.707693	0.089
0.2	0.070394	0.685055	0.061
0.1	0.033903	0.662469	0.034
Complete Polytrope: $n = 3$, $\gamma = 1.40$, $\chi = 0.506897$, $\eta = 0.139909$, $q_1 = 0$[a]			
1.000.....	0.582615	1.96053	...
0.999.....	0.582539	1.92870	33.37
0.995.....	0.582237	1.91235	9.618
0.99	0.581863	1.90377	5.216
0.95	0.578856	1.88718	0.226
0.90	0.575007	1.89169	−0.735
0.85	0.571018	1.90471	−1.187
0.80	0.566858	1.92326	−1.442
0.75	0.562499	1.94622	−1.621
0.70	0.557910	1.97336	−1.752
0.65	0.553055	2.0047	−1.855
0.5	0.536408	2.13049	−2.094
0.4	0.522832	2.25149	−2.209
0.3	0.506020	2.4243	−2.311
0.2	0.483501	2.6998	−2.412
0.1	0.447788	3.26332	−2.515
Complete Polytrope: $n = 3$, $\gamma = 1.45$, $\chi = 0.457161$, $\eta = 0.219411$, $q_1 \sim 0.5$[b]			
1.000.....	0.582615	1.96053	...
0.999.....	0.582457	1.8992	32.19
0.995.....	0.581840	1.86607	10.34
0.99	0.581080	1.84696	6.191
0.95	0.575116	1.79346	1.458
0.90	0.567674	1.77297	0.484
0.85	0.560109	1.76700	0.063
0.80	0.552348	1.76878	−0.188
0.75	0.544333	1.77605	−0.362
0.70	0.536012	1.78787	−0.492
0.65	0.527324	1.80391	−0.596
0.5	0.498334	1.87917	−0.823
0.4	0.475497	1.95856	−0.933
0.3	0.448110	2.0766	−1.033
0.2	0.412845	2.2692	−1.126
0.1	0.360007	2.6670	−1.222
Complete Polytrope $n = 3$, $\gamma = 3/2$, $\chi = 0.424112$, $\eta = 0.284183$, $q_1 = 1.258$			
1.000.....	0.582615	1.96053	...
0.999	0.582353	1.86995	29.73
0.995.....	0.581344	1.82003	9.837
0.99	0.580114	1.79098	6.063
0.95	0.570704	1.70449	1.742
0.90	0.559283	1.66338	0.836
0.85	0.547909	1.64231	0.446
0.80	0.536434	1.63123	0.212
0.75	0.524759	1.62670	0.051
0.70	0.512801	1.62719	−0.071
0.65	0.500479	1.63199	−0.168
0.5	0.460430	1.67117	−0.378
0.4	0.394429	1.80090	−0.566
0.3	0.350412	1.93616	−0.653
0.2	0.287896	2.22106	−0.734
0.1	0.237709	2.57337	−0.810
Complete Polytrope: $n = 3$, $\gamma = 1.55$, $\chi = 0.400584$, $\eta = 0.338114$, $q_1 = 1.630$			
1.000.....	0.582615	1.96053	...
0.999.....	0.582226	1.84115	26.80
0.995.....	0.580749	1.77570	9.086
0.99	0.578974	1.73764	5.695
0.95	0.565734	1.62304	1.772
0.90	0.550115	1.56563	0.946
0.85	0.534876	1.53306	0.588
0.80	0.519747	1.51240	0.374
0.75	0.504572	1.49922	0.226
0.70	.0.489231	1.49149	0.115
0.65	0.473622	1.48819	0.026
0.5	0.424124	1.50131	−0.164
0.4	0.387584	1.53049	−0.257
0.3	0.346287	1.58307	−0.337
0.2	0.296841	1.67773	−0.411
0.1	0.230067	1.88333	−0.488
Complete Polytrope: $n = 3$, $\gamma = 1.60$, $\chi = 0.382996$, $\eta = 0.383812$, $q_1 = 1.890$			
1.000.....	0.582615	1.96053	...
0.999.....	0.582075	1.81334	24.17
0.995.....	0.580062	1.73361	8.332
0.99.....	0.577672	1.68753	5.275
0.95	0.560320	1.54949	1.721
0.90	0.540413	1.47938	0.969
0.85	0.521369	1.43812	0.643
0.80	0.502753	1.41038	0.444
0.75	0.484330	1.39084	0.311
0.70	0.465933	1.3770	0.208
0.65	0.447433	1.36789	0.126
0.5	0.390108	1.36208	−0.046
0.4	0.349028	1.37596	−0.131
0.3	0.303839	1.40861	−0.203
0.2	0.251504	1.47357	−0.270
0.1	0.184126	1.62153	−0.334
Complete Polytrope: $n = 3$, $\gamma = 1.65$ $\chi = 0.369357$, $\eta = 0.423098$, $q_1 = 2.085$			
1.000.....	0.582615	1.96053	...
0.999.....	0.581902	1.78667	21.86
0.995.....	0.579286	1.69392	7.632
0.99	0.576224	1.64087	4.874
0.95	0.554561	1.48342	1.666
0.90	0.530376	1.40341	0.876
0.85	0.507665	1.35561	0.686
0.80	0.485786	1.32254	0.481
0.75	0.464404	1.29827	0.352
0.70	0.443299	1.28006	0.260
0.65	0.422307	1.26643	0.185
0.5	0.358652	1.2463	0.026
0.4	0.314294	1.24883	−0.051
0.3	0.266735	1.2663	−0.115
0.2	0.213369	1.30902	−0.177
0.1	0.147727	1.41373	−0.231
Complete Polytrope: $n = 3$, $\gamma = 5/3$, $\chi = 0.365469$, $\eta = 0.435007$, $q_1 = 2.140$			
1.000.....	0.582615	1.96053	...
0.999.....	0.581939	1.77803	21.15
0.995.....	0.579008	1.68124	7.417
0.99	0.575711	1.62606	4.749
0.95	0.552581	1.46291	1.619
0.90	0.526983	1.38015	0.950
0.85	0.503090	1.33050	0.658
0.80	0.480178	1.29598	0.483
0.75	0.457877	1.27042	0.362
0.70	0.435946	1.25097	0.272
0.65	0.414208	1.2360	0.200
0.5	0.348745	1.21225	0.043
0.4	0.303537	1.21139	−0.029
0.3	0.255463	1.22479	−0.094
0.2	0.202068	1.2610	−0.152
0.1	0.137357	1.35380	−0.207

TABLE 1—*Continued*

ρ_c/ρ_{c0}	x^3	z	ζ_{ad}
Complete Polytrope: $n = 3$, $\gamma = 7/4$, $\chi = 0.349609$, $\eta = 0.487341$, $q_1 = 2.365$			
1.000.....	0.582615	1.96053	...
0.999.....	0.581486	1.73683	18.12
0.995.....	0.577495	1.62175	6.476
0.99	0.572949	1.55729	4.190
0.95	0.542357	1.37061	1.488
0.90	0.509886	1.27690	0.901
0.85	0.480418	1.22021	0.648
0.80	0.452771	1.1800	0.493
0.75	0.426362	1.14942	0.387
0.70	0.400838	1.12518	0.307
0.65	0.375954	1.10556	0.244
0.5	0.303415	1.06618	0.109
0.4	0.255418	1.05266	0.044
0.3	0.206353	1.04944	−0.011
0.2	0.154474	1.06100	−0.061
0.1	0.095936	1.10638	−0.108
Complete Polytrope: $n = 3.5$, $\gamma = 3/2$, $\chi = 0.258732$, $\eta = 0.471306$, $q_1 = 1.880$			
1.000.....	0.651221	2.87505	...
0.999.....	0.650793	2.57309	44.29
0.995.....	0.649213	2.4309	14.75
0.99	0.647347	2.35204	9.200
0.95	0.633843	2.12633	2.880
0.90	0.618304	2.01765	1.575
0.85	0.603333	1.95601	1.014
0.80	0.588578	1.91598	0.681
0.75	0.573840	1.88900	0.451
0.70	0.558979	1.87118	0.280
0.65	0.543872	1.86051	0.143
0.5	0.495903	1.8637	−0.149
0.4	0.419571	1.9585	−0.413
0.3	0.370038	2.0788	−0.529
0.2	0.301142	2.3492	−0.647
0.1	0.246872	2.69383	−0.730
Complete Polytrope: $n = 3.5$, $\gamma = 5/3$, $\chi = 0.240133$, $\eta = 0.639645$, $q_1 = 2.903$			
1.000.....	0.651221	2.87505	...
0.999.....	0.649893	2.3574	25.61
0.995.....	0.645412	2.13881	9.069
0.99	0.640455	2.02388	5.822
0.95	0.608421	1.71645	2.023
0.90	0.575388	1.57420	1.206
0.85	0.545741	1.49181	0.858
0.80	0.515348	1.43031	0.629
0.75	0.491600	1.39294	0.500
0.70	0.466009	1.36037	0.390
0.65	0.440981	1.33472	0.303
0.5	0.367245	1.28660	0.118
0.4	0.317478	1.27350	0.028
0.3	0.265397	1.2762	−0.048
0.2	0.208433	1.30273	−0.118
0.1	0.140492	1.38513	−0.184
Complete Polytrope: $n = 3.5$, $\gamma = 7/4$, $\chi = 0.233147$, $\eta = 0.697961$, $q_1 = 3.159$			
1.000.....	0.651221	2.87505	...
0.999.....	0.649270	2.26767	20.92
0.995.....	0.642974	2.02469	7.542
0.99	0.636219	1.90039	4.901
0.95	0.594624	1.57664	1.762
0.90	0.553630	1.42968	1.083
0.85	0.517870	1.34436	0.787
0.80	0.482021	1.28015	0.592
0.75	0.454520	1.24056	0.483
0.70	0.425349	1.20535	0.390
0.65	0.397271	1.17680	0.316
0.5	0.317087	1.11763	0.158
0.4	0.265154	1.09429	0.082
0.3	0.212835	1.08269	0.019
0.2	0.158268	1.08659	−0.039
0.1	0.097550	1.12416	−0.094
Complete Polytrope: $n = 4$, $\gamma = 3/2$, $\chi = 0.140415$, $\eta = 0.738720$, $q_1 = 2.864$			
1.000.....	0.725067	4.75871	...
0.999.....	0.724293	3.74332	54.85
0.995.....	0.721647	3.36009	18.65
0.99	0.718683	3.16435	11.74
0.95	0.698968	2.65770	3.829
0.90	0.677885	2.43381	2.180
0.85	0.658391	2.30895	1.493
0.80	0.639698	2.2262	1.071
0.75	0.621412	2.16770	0.783
0.70	0.603280	2.12494	0.572
0.65	0.585114	2.0936	0.404
0.5	0.528785	2.05165	0.034
0.4	0.442175	2.10507	−0.284
0.3	0.387396	2.20843	−0.432
0.2	0.312626	2.46229	−0.576
0.1	0.254704	2.7979	−0.661
Complete Polytrope: $n = 4$, $\gamma = 5/3$, $\chi = 0.139995$, $\eta = 0.938049$, $q_1 = 4.125$			
1.000.....	0.725067	4.75871	...
0.999.....	0.722589	3.22027	22.79
0.995.....	0.715222	2.74556	10.03
0.99	0.707670	2.52250	6.510
0.95	0.663689	1.99238	2.324
0.90	0.621912	1.77272	1.410
0.85	0.585936	1.65096	1.014
0.80	0.553186	1.56891	0.775
0.75	0.522516	1.50858	0.609
0.70	0.493275	1.46201	0.485
0.65	0.465034	1.42508	0.387
0.5	0.383474	1.35258	0.176
0.4	0.329540	1.32766	0.075
0.3	0.273881	1.32049	−0.011
0.2	0.213796	1.33793	−0.089
0.1	0.143095	1.41117	−0.168
Complete Polytrope: $n = 4$, $\gamma = 7/4$, $\chi = 0.137884$, $\eta = 1.00702$, $q_1 = 4.435$			
1.000.....	0.725067	4.75871	...
0.999.....	0.721419	3.02329	21.87
0.995.....	0.711241	2.53330	8.096
0.99	0.701184	2.30959	5.325
0.95	0.645497	1.79127	1.965
0.90	0.594920	1.57994	1.223
0.85	0.552521	1.46261	0.894
0.80	0.514693	1.38309	0.696
0.75	0.479871	1.32400	0.558
0.70	0.447188	1.27775	0.455
0.65	0.416092	1.24035	0.373
0.5	0.328890	1.16227	0.198
0.4	0.273452	1.12989	0.114
0.3	0.218294	1.11074	0.043
0.2	0.161426	1.10791	−0.021
0.1	0.098877	1.13876	−0.083

[a] No tangent point exists since ζ_{ad}, for large perturbations, is less than $-5/3$.
[b] Tangent point is beyond the range of perturbations calculated.

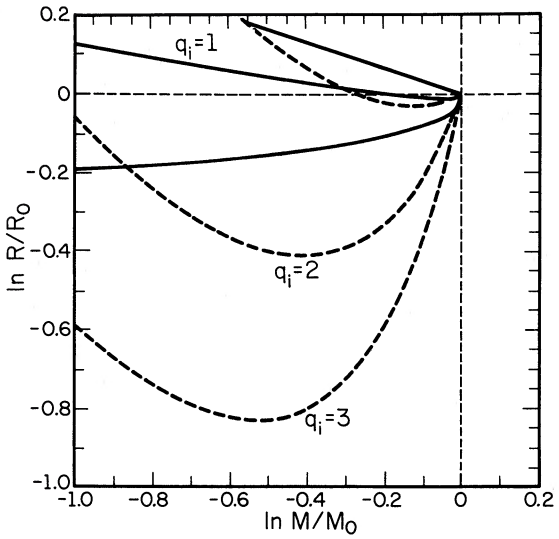

FIG. 2.—Adiabatic response curves for the $n = 3/2$ complete polytropes (*solid lines, top to bottom:* $\gamma = 5/3, 7/4, 2$). Heavy dashed lines are Roche lobe curves for three initial mass ratios.

coordinates for the central pressure and density in terms of the final mass and radius (Chandrasekhar 1939, p. 99), we find the limiting mass-radius relation for $M \ll M_0$:

$$\frac{R}{R_0} = \left(\frac{m+1}{n+1}\right)^{m/(3-m)} \left(\frac{\xi_m}{\xi_n}\right)^{(1+m)/(3-m)} \times \left(\frac{\phi'_m}{\phi'_n}\right)^{(m-1)/(3-m)} \left(\frac{M}{M_0}\right)^{(1-m)/(3-m)} \equiv \chi(n, m)\left(\frac{M}{M_0}\right)^{(1-m)/(3-m)}, \quad (18)$$

where $m = 1/(\gamma - 1)$, and ξ_k is the independent radial variable and $\phi'_k = d\phi/d\xi$ is the derivative of the Lane-Emden solution of degree k, both evaluated at the surface of the polytrope. The coefficients for this asymptotic mass-radius relationship for large perturbations are included in Table 1 as the parameter χ.

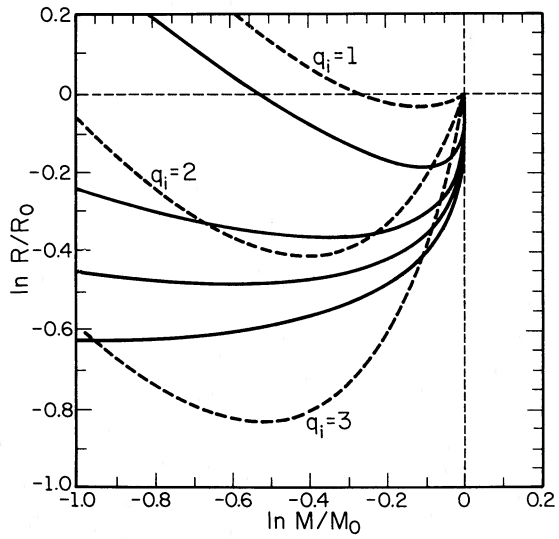

FIG. 3.—Adiabatic response curves for the $n = 3$ complete polytropes (*solid lines, top to bottom:* $\gamma = 3/2, 1.60, 5/3, 7/4$). Heavy dashed lines are Roche lobe curves for three initial mass ratios.

The asymptotic adiabatic response of polytropes to mass loss in the limit of small perturbations was studied analytically by Paczyński (1965) and numerically by Heisler and Alcock (1986). Paczyński showed that the radii of stars with subadiabatic polytropic envelopes ($n_e > 1/[\gamma_e - 1]$) vary as

$$\frac{\Delta R}{R_0} = [1 - \alpha(\gamma_e, n_e)] \frac{n+1}{4\pi} \left(\frac{GM_0}{4\pi K_e R_0}\right)^{-n_e/(n_e+1)} \times R_0^{(n_e-2)/(n_e+1)} \left(\frac{\Delta M}{M_0}\right)^{1/(n_e+1)}, \quad (19)$$

where $\Delta R = R_0 - R$, $\Delta M = M_0 - M$, and K_e is the polytropic constant characterizing the unperturbed envelope. The function $\alpha(\gamma_e, n_e)$ is obtained by matched series solutions, yielding

$$\alpha(\gamma_e, n_e) = 2^{1/(n_e+1)} \sum_{k=0}^{\infty} \frac{a_{k+1}}{2^{k+1}[(k+1)(n_e+1) - 1]} + \frac{2^{1/\gamma}}{n_e+1} \sum_{k=0}^{\infty} \frac{b_k}{2^{k+1}[k + (\gamma-1)/\gamma]} - \frac{1}{n_e+1} \sum_{k=0}^{\infty} \frac{b_k}{2^{k+1}(k+1)}, \quad (20)$$

where $a_0 = 1$, $a_k = a_{k-1}(k - 1 + 1/\gamma)/k$, and $b_0 = 1$, $b_k = b_{k-1}[k + 1/(n_e + 1)]/k$. For complete polytropes, equation (19) reduces to

$$\frac{\Delta R}{R_0} = (1 - \alpha)(n+1)^{1/(n+1)} \xi^{n-1} \times \left(-\frac{d\phi_n}{d\xi}\right)^{-(n-1)/(n+1)} \left(\frac{\Delta M}{M_0}\right)^{1/(n+1)} \equiv \eta(n, \gamma)\left(\frac{\Delta M}{M_0}\right)^{1/(n+1)}, \quad (21)$$

where ξ_n and ϕ'_n are defined as in equation (18) above. The coefficients for this asymptotic relationship for small perturbations are included in Table 1 as the parameter η.

The numerical results of Heisler and Alcock are in reasonably good agreement with the analytic results by Paczyński. In fact, our own calculations, which are in very good agreement with those of Heisler and Alcock, asymptotically approach Paczyński's relationship, but show that higher order corrections rapidly become important as perturbations exceed $\sim 10^{-3}$ of the central density (or even less, for the polytropes of largest n considered here). The consequence of equations (19) and (21) is that the radius-mass exponent, ζ_{ad}, becomes asymptotically infinite for unperturbed polytropes with $n > 1(\gamma - 1)$.

III. COMPOSITE POLYTROPES

The composite polytropes are constructed in the same fashion as the complete polytropes. A core of degree n_c is calculated satisfying equations (7) and (12). At a preselected interface position, $x_i < x_{\text{surface}}$, we continue into an envelope of degree n_e. The fitting conditions for the two solutions are found by demanding continuity of mass, pressure, radius, and density. They are

$$\frac{x_c}{\theta_c}\frac{d\theta_c}{dx_c} = \frac{x_e}{\theta_e}\frac{d\theta_e}{dx_e}, \quad (22)$$

$$x_c\, \theta_c^{(n_c-3)/6(n_c+1)} = x_e\, \theta_e^{(n_e-3)/6(n_e+1)}. \quad (23)$$

We are free to choose one of the envelope parameters, x_e, θ_e, or $d\theta_e/dx_e$, in order to fix the other two. For our purposes, we choose to maintain continuity in the mass coordinate, x, and so adopt the conditions:

$$x_e = x_c \,, \tag{24}$$

$$\theta_e = \theta_c^{\lambda} \,, \tag{25}$$

$$\frac{d\theta_e}{dx_e} = \frac{d\theta_c}{dx_c}\,\theta_c^{\lambda-1} \,, \tag{26}$$

where

$$\lambda \equiv \frac{n_c - 3}{n_e - 3}\frac{n_e + 1}{n_c + 1} \,. \tag{27}$$

Thus

$$z_e = z_c\,\theta_c^{(1-\lambda)/4} \,. \tag{28}$$

The scaling constants a, P_e, and K in the envelope are related to those in the core as follows:

$$a_e = a_c \,, \tag{29}$$

$$P_e = P_c\,\theta_c^{1-\lambda} \,, \tag{30}$$

$$K_e = K_c\left(\frac{K_c}{P_c\,\theta_c}\right)^{[(n_c/n_e)(n_e+1)/(n_c+1)]-1} \,, \tag{31}$$

where θ_c is evaluated at the core-envelope interface. The envelope is then integrated to the surface, where $\theta_e = 0$. If $n_c > n_e$, the absolute values of the first and second derivatives of the envelope solution increase at the interface. The result is a smaller total mass than for the complete polytrope of degree n_c. If $n_c < n_e$, the opposite occurs. The continuity requirements of pressure and radius for the perturbed polytrope result in the trivial relations:

$$\omega_e = \omega_c \,, \tag{31a}$$

$$\frac{d\omega_e}{dx_e} = \frac{d\omega_c}{dx_c} \,. \tag{31b}$$

Finally, if $\gamma_e = \gamma_c$, $d^2\omega_e/dx_e^2 = d^2\omega_c/dx_c^2$, and if $\gamma_e > \gamma_c$, $d^2\omega_e/dx_e^2 < d^2\omega_c/dx_c^2$ ($\gamma_e < \gamma_c$ being physically excluded by convective instability of the boundary).

The construction of the composite polytropes is intended to approximate the radiative cores and convective envelopes of lower main-sequence stars. We consider only one combination of indices: $n_c = 3$, $n_e = 3/2$, and $\gamma_c = \gamma_e = 5/3$. This choice simplifies the matching conditions to $x_e = x_c$, $\theta_e = 1$, $d\theta_e/dx_e = \theta_c^{-1}d\theta_c/dx_c$, $d^2\theta_e/dx_e^2 = \theta_c^{-1}d^2\theta_c/dx_c^2$, $z_e = z_c\,\theta_c^{1/4}$, $a_e = a_c$, $P_e = P_c\,\theta_c$, and $K_e = K_c^{5/4}(P_c\,\theta_c)^{-1/4}$. Only relatively small perturbations need be considered because sufficiently large perturbations remove the entire envelope, leaving a core identical to a perturbed $n = 3$, $\gamma = 5/3$ complete polytrope with the same value of ω_0. However, additional values of ω_0 near unity were calculated to explore in more detail the cases with small envelopes. We calculated six models with interface mass fractions of 0.263, 0.546, 0.688, 0.817, 0.919, 0.966, and 0.982. The results of these calculations are given in Table 2, which follows a format paralleling that of Table 1. In Table 2, the subscript i denotes values of the core solution at the core-envelope interface. The dimensionless surface radius, z_e, has been rescaled by a factor of $\theta_i^{-1/4}$ in order to maintain continuity across this boundary (see eq. [28]).

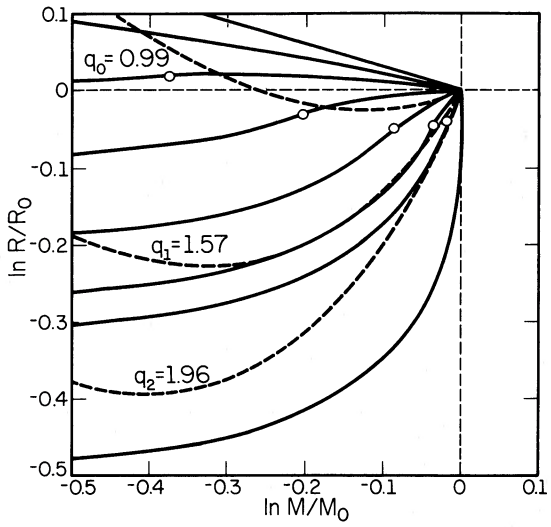

FIG. 4.—Adiabatic response curves for the composite polytropes (*solid lines*). Circles indicate the interface locations between the radiative core and the convective envelope (from top: $m_c = 0.263$, 0.546 [first two circles are off the scale], 0.688, 0.817, 0.919, 0.966, and 0.982). Bottom solid curve is the fully radiative model ($n = 3$, $\gamma = 5/3$). Heavy dashed lines illustrate Roche lobe curves for three initial mass ratios corresponding to three critical values: initial dynamical stability (q_0, for $m_c = 0.919$), initial dynamical instability with an interval of slower mass loss (q_1, for $m_c = 0.966$), and dynamical instability until overcome by adiabatic reexpansion (q_2, for $m_c = 0.982$).

The behavior of these models is a competition between the tendencies of each region to contract or expand. As shown in Figure 4, the initial response of equilibrium models ranges from an adiabatic exponent of $-\frac{1}{3}$, in the completely convective limit, to the infinite slope of the purely radiative model, as the initial envelope becomes smaller. Along a given mass-loss sequence, the adiabatic radius-mass exponent increases as the envelope mass becomes smaller, reaching a maximum as the surface reaches the core boundary, whereupon the appropriate response for the radiative case takes over.

Paczyński (1965) found that, in the limit of $n_e \to 1/(\gamma_e - 1)$, $\alpha(\gamma_e, n_e)$ goes to unity (see eqs. [19] and [20]), and the technique employed above to calculate the asymptotic adiabatic response of a polytropic envelope fails. This is not surprising, since we know that, in the case of complete polytropes with $n = 1/(\gamma - 1)$, the polytrope responds homologously to mass loss, with $(\Delta R/R_0) \sim (\Delta M/M_0)$, rather than $(\Delta R/R_0) \sim (\Delta M/M_0)^{1/(n+1)}$ as arises from lowest order perturbation theory (eq. [19]). From a fresh approach to the problem of a star with an isentropic envelope, he deduced that the asymptotic response for infinitesimal mass loss was in this case $\zeta_{ad} \to (\gamma_e - 2)/(3\gamma_e - 4)$, just as for complete polytropes with $n = 1/(\gamma - 1)$, regardless of the depth of the envelope or the nature of the core.

Our calculations indicate that this behavior holds only in the limit of vanishingly small core mass. Finite core masses produce $\zeta_{ad} > -\frac{1}{3}$ (for an envelope with $\gamma = 5/3$), with the difference increasing monotonically with an increasing fractional core mass. The discrepancy apparently originates from Paczyński's implicit assumption that the pressure variation at the base of the isentropic envelope is negligible for sufficiently small perturbations. This assumption is justified for the subadiabatic envelopes discussed above in the context of complete polytropes because the stellar radius varies with mass as $\delta R/R \approx (\delta M/M)^{1/(n+1)}$. But the variations in radius at a given mass

TABLE 2

ADIABATIC RESPONSES OF MASS-LOSING COMPOSITE POLYTROPES

ρ_c/ρ_{c0}	x^3	$z_e\theta_i^{-1/4}$	ζ_{ad}
Composite Polytrope: $x_i = 0.500$, $\theta_i = 0.383542$, $q_0 = 0.645$			
1.0000.....	0.475195	0.948743	−0.310
0.9995.....	0.475070	0.948831	−0.309
0.999	0.474944	0.948906	−0.309
0.995	0.473937	0.949519	−0.308
0.99	0.472676	0.950295	−0.308
0.95	0.462473	0.956689	−0.306
0.90	0.449420	0.965123	−0.306
0.85	0.436008	0.974107	−0.305
0.80	0.422206	0.983705	−0.304
0.75	0.407977	0.994016	−0.304
0.50	0.328620	1.06074	−0.298
0.25[a]	0.226194	1.18212	−0.278
Composite Polytrope: $x_i = 0.662$, $\theta_i = 0.126342$, $q_0 = 0.668$			
1.0000.....	0.531634	1.09623	−0.217
0.9995.....	0.531473	1.09629	−0.216
0.999	0.531311	1.09636	−0.216
0.995	0.530021	1.09694	−0.215
0.99	0.528406	1.09768	−0.215
0.95	0.515350	1.10356	−0.213
0.90	0.498692	1.11121	−0.209
0.85	0.481634	1.11924	−0.205
0.80	0.464145	1.12763	−0.199
0.75	0.446192	1.13641	−0.193
0.7	0.427735	1.14563	−0.189
0.6	0.408732	1.15529	−0.181
0.5	0.347903	1.18704	−0.155
0.4[a]	0.303515	1.20881	−0.115
Composite Polytrope: $x_i = 0.725$, $\theta_i = 0.0574387$, $q_0 = 0.733$			
1.0000.....	0.553608	1.19526	−0.119
0.9995.....	0.553421	1.19530	−0.119
0.999	0.553234	1.19534	−0.119
0.995	0.551736	1.19572	−0.118
0.99	0.549861	1.19620	−0.117
0.95	0.534739	1.20000	−0.110
0.90	0.515530	1.20463	−0.101
0.85	0.495968	1.20910	−0.090
0.80	0.476038	1.21328	−0.078
0.75	0.455730	1.21702	−0.063
0.7	0.435036	1.22010	−0.045
0.6[a]	0.392498	1.22257	0.011
Composite Polytrope: $x_i = 0.775$, $\theta_i = 0.0203991$, $q_0 = 0.814$			
1.0000.....	0.569430	1.31599	0.056
0.9995.....	0.569209	1.31597	0.056
0.999	0.568987	1.31594	0.055
0.999	0.567216	1.31571	0.054
0.99	0.565000	1.31508	0.051
0.95	0.547227	1.31245	0.081
0.90	0.524907	1.30721	0.112
0.85	0.502517	1.29981	0.149
0.80[a]	0.480125	1.28983	0.189
Composite Polytrope: $x_i = 0.810$, $\theta_i = 0.00499644$, $q_0 = 0.991$			
1.0000.....	0.578491	1.46059	0.437
0.9995.....	0.578225	1.46018	0.437
0.999	0.577959	1.46000	0.438
0.995	0.575834	1.45766	0.442
0.99	0.573184	1.45466	0.448
0.98	0.567905	1.44851	0.468
0.97	0.562656	1.44207	0.493
0.95.....	0.552256	1.42807	0.554
0.93	0.542005	1.41222	0.648
0.91[a]	0.531932	1.39299	0.835
Composite Polytrope: $x_i = 0.825$, $\theta_i = 0.00129104$, $q_0 = 1.281$, $q_1 = 1.571$, $q_2 = 1.604$			
1.0000.....	0.581394	1.57679	1.063
0.9995.....	0.581090	1.57591	1.066
0.999	0.580786	1.57503	1.069
0.995	0.578364	1.56791	1.104
0.99	0.575361	1.55872	1.156
0.98	0.569447	1.53913	1.302
0.97[a]	0.563663	1.51726	1.515
Composite polytrope: $x_i = 0.830$, $\theta_i = 0.000503824$, $q_0 = 1.665$, $q_1 = 1.694$, $q_2 = 1.958$			
1.0000.....	0.582119	1.64452	1.888
0.9995.....	0.581792	1.64281	1.807
0.999	0.581465	1.64117	1.766
0.995	0.578871	1.62737	1.727
0.992	0.576952	1.61652	2.036
0.99[a]	0.575684	1.60896	2.826

[a] Data for smaller values of ρ_c/ρ_{c0} can be found in the entry for the $n = 3, \gamma = 5/3$ complete polytrope in Table 1.

coordinate scale linearly with variations in pressure, which in turn vary linearly with total mass: $\delta r/r \sim \delta P/P \sim \delta M/M$. Thus, for small enough perturbations, the lowest order radial response of the star can be confined to an arbitrarily small region near the surface: $\delta r/r \sim (\delta R/R)^{n+1}$. If the envelope is isentropic however, the variation in stellar radius is *linearly* proportional to the variation in mass, $\delta R/R \sim \delta M/M$, and thus $\delta r/r \sim \delta R/R$—i.e., the radial response is an integral response through the entire interior.

Rappaport, Verbunt, and Joss (1983) have also nominally investigated the adiabatic responses of composite polytropes. They assume that each region of the star responds homologously and permit the core-envelope boundary to move so as to ensure global conservation of energy. Strictly speaking, neither of these assumptions is valid: the response is not homologous in a truly radiative core, and the core-envelope boundary is fixed by the entropy profile, which is invariant by the assumption of adiabaticity. Nevertheless, their results for marginal stability do not differ greatly from ours, except for small envelope masses, and they follow the same qualitative trends. We attribute this success to the fact that, unless the envelope is thin, entropy gradients within the core are sufficiently mild that departures from homologous response are small.

IV. CONDENSED POLYTROPES

The condensed polytropes differ from the complete polytropes in their boundary conditions. Where we had $m(0) = 0$, we now have a finite point mass at the center. In an Eulerian coordinate system where $P/\rho \sim \phi$, $r \sim \xi$, $m \sim -\xi^2 d\phi/d\xi$, the function ϕ satisfies the standard form of the Lane-Emden equation, but it is one of the singular solutions. These solutions

are parameterized by the conditions at the surface where $\phi = 0$. Complete polytropes obey the following relation, which is homologously invariant (see Osterbrock 1953; Schwarzschild 1958):

$$(n+1)^n \xi_s^{n+1} \left(-\frac{d\phi}{d\xi} \right)_{\xi=\xi_s}^{n-1} = 4\pi G^n M^{n-1} R^{3-n} K^{-n} \equiv E_{\max} . \quad (33)$$

For the same ξ_s, a singular solution can be found by substituting $E < E_{\max}$, so that $d\phi_s/d\xi > (d\phi_s/d\xi)_0$. These are the M-solutions described by Chandrasekhar (1939, p. 120) and tabulated by Härm and Schwarzschild (1955, Table 15) for the case of an $n = 3/2$ envelope. The solution has a finite value for $-\xi^2 d\phi/d\xi$ at the origin, implying a nonzero core mass. The core and total masses, and therefore the core mass fraction, m_c, are functions only of E. As E decreases from $E_{\max}$ to 0.0, m_c increases from 0.0 to 1.0.

For our purposes, we are interested in condensed polytropes with $n = 3/2$, $\gamma = 5/3$ (convective) envelopes. In this case, $E_{\max} = 45.4808$. These models serve as approximations to giant branch stars with degenerate cores. The dependence of m_c on E is given in this case in Table 3, which adopted in large measure from Table 1 of Paczyński and Sienkiewicz (1972).

A model for a mass-losing condensed polytrope is constructed with an initial core mass fraction, m_{ci}, and a corresponding E_i. As mass is removed from the outer layers, m_c becomes larger, so E decreases. The behavior of the radius is determined by equation (33), where K remains constant, if $n = 1/(\gamma - 1)$ as it does here. Because $m_c = m_{c0}(M/M_0)^{-1}$, we have from equation (33):

$$\ln \frac{R}{R_0} = -\frac{1}{3} \ln \frac{M}{M_0} + \frac{2}{3} \ln \frac{E}{E_0} , \quad (34)$$

TABLE 3

CONDENSED POLYTROPES: $n_e = 3/2$, $\gamma_e = 5/3$

E	m_c	$\frac{dm_c}{dE}$	ζ_{ad}	q_c
0	1.0000	−0.0497	∞	∞
2	0.9050	−0.0454	6.310	3.735
4	0.8182	−0.0414	2.957	2.163
6	0.7389	−0.0379	1.831	1.638
8	0.6662	−0.0348	1.261	1.373
10	0.5995	−0.0319	0.919	1.214
12	0.5384	−0.0292	0.689	1.108
14	0.4823	−0.0269	0.521	1.030
16	0.4307	−0.0247	0.393	0.970
18	0.3833	−0.0227	0.291	0.923
20	0.3396	−0.0210	0.206	0.884
22	0.2993	−0.0193	0.136	0.851
24	0.2662	−0.0178	0.075	0.823
26	0.2279	−0.0165	0.021	0.798
28	0.1962	−0.0153	−0.027	0.776
30	0.1668	−0.0141	−0.071	0.755
32	0.1396	−0.0131	−0.111	0.737
34	0.1144	−0.0121	−0.148	0.720
36	0.0910	−0.0113	−0.184	0.703
38	0.0693	−0.0105	−0.217	0.688
40	0.0490	−0.0098	−0.250	0.673
42	0.0301	−0.0091	−0.281	0.658
44	0.0124	−0.0087	−0.312	0.644
45.4808	0.0000	−0.0083	−0.333	0.634

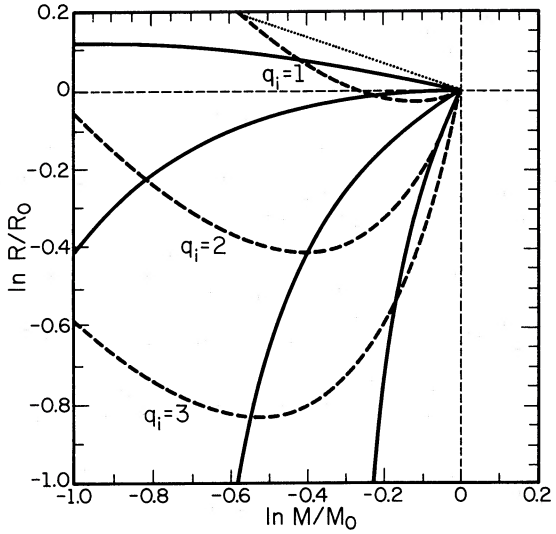

FIG. 5.—Adiabatic response curves for the condensed polytropes (solid lines for core mass fractions of 0.10, 0.25, 0.50, 0.75, from top to bottom). Dotted line represents the limiting response ($\zeta_{ad} = -\frac{1}{3}$) as $m_c \to 0$. Heavy dashed lines are Roche lobe curves for three initial mass ratios.

$$\zeta_{ad} = -\frac{1}{3} \left(1 + 2 \frac{d \ln E}{d \ln m_c} \right) . \quad (35)$$

The values of ζ_{ad} are tabulated in the fourth column of Table 3.

Figure 5 illustrates the results for four initial core mass fractions ranging from 0.10 to 0.75. (These are actually portions of a single fiducial curve, since the E-models are a single-parameter family of models.) In the limit of vanishingly small core mass ($m_c \to 0$) the response asymptotically approaches that of an $n = 3/2$, $\gamma = 5/3$ polytrope, as one would expect. For small core masses, the expansion in response to mass-loss characteristic of that limit is also apparent, but as the envelope mass is stripped to the point where the core mass fraction exceeds a critical value ($m_c > 0.2139$, corresponding to $E > 26.854$), the envelope begins to contract, a contraction which becomes arbitrarily steep as the envelope mass vanishes.

The asymptotic behavior of condensed polytropes in the limit of vanishingly small envelope mass ($M_e \ll M$, i.e., $m_c \to 1$) can be calculated by integrating the equation of hydrostatic equilibrium inward from the surface. One finds

$$\rho(r) = \left[\frac{GM}{K(n+1)} \right]^n (r^{-1} - R^{-1})^n , \quad (36)$$

from which it follows that (for $n < 3$)

$$M_e = \int_0^R 4\pi r^2 \rho dr = \frac{2\pi}{3} \Gamma(n+1)\Gamma(3-n) \left[\frac{GM}{K(n+1)} \right]^n R^{3-n} . \quad (37)$$

Substitution of equation (33) gives

$$M_e/M = 1 - m_c = \tfrac{1}{6}(n+1)^{-n}\Gamma(n+1)\Gamma(3-n)E , \quad (38)$$

or (for $n = 3/2$),

$$m_c = 1 - \frac{\pi}{16} \left(\frac{2}{5} \right)^{3/2} E . \quad (39)$$

The adiabatic radius-mass exponent becomes asymptotically

$$\zeta_{\rm ad} = \frac{1}{3-n}\left(1-n+\frac{m_c}{1-m_c}\right). \quad (40)$$

It should be emphasized that the condensed polytropes examined here adequately describe red giant stars only to the extent that their envelopes follow the classical perfect gas law (with $\gamma = 5/3$). Very luminous red giants and asymptotic branch giants have convective envelopes in which radiation pressure is important or even dominant, and hence depart significantly from a $\gamma = 5/3$ adiabat. Also the mass density becomes so low that convection becomes significantly superadiabatic, $n < 1/(\gamma_e - 1)$.

V. DISCUSSION

In order to place the adiabatic responses of polytropes into the context of mass transfer in binary systems, we must calculate the response of the Roche lobe. Let us assume conservation of total mass and orbital angular momentum, as well as the usual assumptions involved in the adoption of the Roche geometry. The resulting dependence of the separation upon the mass ratio goes as $q^2(1+q)^{-4}$, where $q \equiv M_1/M_g$ is the mass ratio (loser/gainer). The volume equivalent Roche lobe radius can then be approximated by (Eggleton 1983)

$$R_L = \frac{J^2}{GM^3}\frac{0.49q^{2/3}}{0.60q^{2/3}+\ln(1+q^{1/3})}\frac{(1+q)^4}{q^2}. \quad (41)$$

The value of R_L, normalized to the initial value R_{L0}, thus depends only upon the current mass ratio, q, and the initial mass ratio, q_i. The resulting curves for $q_i = 1.0$, 2.0, and 3.0 have been included for comparison in Figures 2–4. The radius-mass exponent for the Roche lobe is

$$\zeta_L = (1+q)\frac{d\ln R_L}{d\ln q}. \quad (42)$$

The question of whether dynamical time scale mass transfer occurs depends on whether, at any point in the evolution of a donor star, $R_{\rm ad} > R_L$. For the initial dynamical stability of a star just filling its Roche lobe ($R = R_L$), it suffices to have $\zeta_L < \zeta_{\rm ad}$. The tangency condition, $\zeta_L = \zeta_{\rm ad}$ at $M/M_0 = 1$, thus defines a critical mass ratio, q_0, above which a system is initially unstable to dynamical time scale mass exchange. In fact, q_0 is finite for our polytropic models only if the surface layers are isentropic; a subadiabatic (radiative) surface leads formally to $q_0 \to +\infty$ (see eq. [19]). This behavior is an artifact of the polytropic assumption that $P \to 0$ at the surface, which produces an infinite surface entropy (eq. [17]). In real stars, this singularity is removed, but q_0 will nevertheless be very large if the surface layers are radiative.

While they tend to be strongly stable against dynamical time scale mass transfer initially, stars with subadiabatic envelopes may ultimately reexpand in response to rapid mass loss. This reexpansion is a consequence of stripping the star to a nearly isentropic core. As a result, it may occur that $R_{\rm ad}$ initially contracts much more rapidly than R_L (continued mass transfer in this case being driven by thermal relaxation in the envelope of the donor star), but the growing difference is eventually slowed and is overtaken by the contraction of R_L. Thus a system initially stable against dynamical time scale mass transfer may later, upon loss of a finite amount of mass, become unstable in this mode. An example of the phenomenon may be seen in Figure 3, where the $R_L(M/M_0)$ curve for $q_i = 2$ lies above $R_{\rm ad}(M/M_0)$ for $\log M/M_0 > -0.23$ but falls below the latter in the range $-0.23 > \log M/M_0 > -0.67$, before again growing larger for smaller masses yet. The model calculation by Webbink (1977) discussed in the Introduction is a more realistic example of this phenomenon. To the extent that we may neglect thermal relaxation within the deep interior of the mass-losing star during the initial slower-than-dynamical time scale mass-loss phase (see again the discussion of Fig. 1), we can estimate the critical initial mass ratio, q_1, above which this delayed dynamical mass transfer occurs by identifying it with that R_L curve which is just tangent at one point, where $M/M_0 < 1$, with $R_{\rm ad}$ ($\zeta_L = \zeta_{\rm ad}$ at this point), and for which $R_L = R_{\rm ad}$ at $M/M_0 = 1$.

If the dependence of $\zeta_{\rm ad}$ on remnant mass fraction, M/M_0, is sufficiently complicated, it is possible for the R_L and $R_{\rm ad}$ curves to intersect at more than two points (including the starting point at $M/M_0 = 1$). In this case, it is possible to define additional critical mass ratios. Among our simplified models, this circumstance arises only for composite polytropes with small envelope masses. Here we can identify four distinct types of evolution: For sufficiently small initial mass ratios ($q_i < q_0$), mass loss from the donor star is always slower than dynamical. For higher initial mass ratios ($q_1 > q_i > q_0$), the initial mass transfer is unstable until $R_{\rm ad} < R_L$ from the adiabatic contraction of the radiative core. (This was the outburst mechanism for U Gem stars originally proposed by Paczyński 1965.) For somewhat higher initial mass ratios ($q_2 > q_i > q_1$), the later adiabatic expansion of the core leads to a second phase of dynamical time scale mass transfer, followed ultimately by stability, for small enough M/M_0. Finally, for the most extreme initial mass ratios ($q_i > q_2$), the interval of thermal time scale mass loss disappears and dynamical time scale mass loss occurs until finally stabilized at even smaller values of M/M_0. (Whether mass and angular momentum are likely to be conserved if $q_i > q_0$ is debatable. If this condition is strongly violated, common envelope evolution may ensue; see below.)

The critical mass ratios defined in this way are included in Table 2, as appropriate. It should be emphasized that these estimates neglect the possible stabilizing effect of thermal relaxation in stellar interiors. For initial stability (q_0), those effects are probably of minimal importance, but in cases of delayed dynamical mass transfer (q_1), the onset of instability may be delayed or avoided altogether if the initial mass transfer time scale is sufficiently slow. Adiabatic estimates of q_1 and q_2 should therefore be regarded as lower limits to the true thresholds.

What then is the significance of these results? Stars of intermediate or low mass ($M \leq 10\ M_\odot$), on or very near the zero-age main sequence, can be well approximated by complete polytropes ($n = 3/2$, $\gamma = 5/3$ for $0.1 \leq M/M_\odot \leq 0.3$; $n = 3$, $\gamma = 5/3$ for $1 \leq M/M_\odot \leq 10$) or by composite polytropes ($n_e = 3/2$, $n_c = 3$, $\gamma = 5/3$ for $0.3 \leq M/M_\odot \leq 1$). This correspondence can be seen in Figure 6, where the ratio of central to mean densities (a measure of the effective polytropic degree), the central value of the adiabatic index, and the core mass fraction for a model zero-age main sequence of solar metallicity are plotted as functions of mass. Our polytropic models are less satisfactory approximations for upper main-sequence stars, because the ratio of radiation to gas pressure varies significantly along an adiabatic mass-loss sequence (as a consequence of which γ varies as well), and because very massive stars have very extensive convective cores.

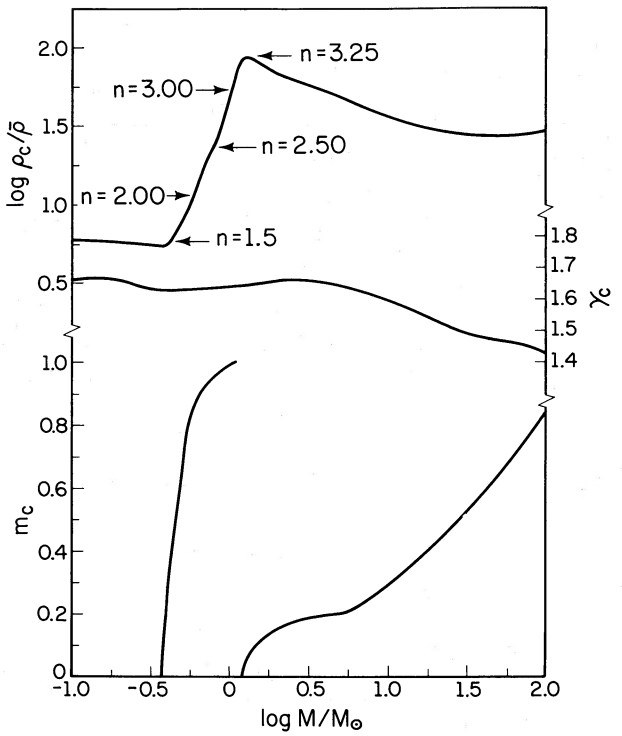

FIG. 6.—Properties of detailed zero-age main-sequence models (of solar composition), for comparison with our polytropic models. Plotted are the ratio of central density to mean density (with the corresponding values indicated for the equilibrium complete polytropes), the central adiabatic index, and the core mass fraction (radiative for $M < 1.1\ M_\odot$, and convective for $M > 1.1\ M_\odot$).

We see that marginal stability against dynamical time scale mass transfer poses a severe constraint on allowable mass ratios among lobe-filling lower main-sequence stars which are fully convective, or have deep convective envelopes. In fact, the thermal equilibrium radius-mass relationship for these stars ($\zeta_{th} \approx 1$) is such that stars with radiative cores of mass fraction $m_c \leq 0.964$, corresponding roughly to $M \leq 0.84\ M_\odot$, have $\zeta_{ad} < \zeta_{th}$ (see Fig. 2.2.3 in Webbink 1985). For these stars, considerations of stability against thermal–time scale mass transfer are irrelevant: they become unstable to dynamical time scale mass transfer before the thermal time scale stability criterion is violated. Thus, for example, as recognized by Tutukov, Fedorova, and Yungel'son (1982), dynamical equilibrium constrains allowable white dwarf masses in cataclysmic variables even more strongly than thermal equilibrium (Ritter 1976).

As one proceeds up the main sequence, ζ_{ad} and q_0 increase very rapidly for unperturbed stars. Above $\sim 1\ M_\odot$, lobe-filling stars are initially stable against dynamical time scale mass transfer for any reasonable mass ratio. However, the polytropic models suggest, as the detailed evolutionary calculation by Webbink (1977) demonstrates, that delayed dynamical time scale mass transfer may occur if the initial mass ratio is moderately extreme: $q_i > q_1$ ($= 2.14$ for an $n = 3$, $\gamma = 5/3$ polytrope). Whether this actually occurs in reality depends on a number of factors, not the least of them being the nature of the accreting star. In fact, if that accreting star is itself unevolved, it will almost certainly swell into contact before dynamical instability is reached, unless it is very low in mass (see, for example, the evolutionary calculations in Webbink 1976). If, on the other hand, the accreting object is compact (a white dwarf, neutron star, or black hole), it is at least conceivable that this sort of transition could occur over a wide range of circumstances.

What, then, of evolved stars? The thermal evolution of evolving main-sequence stars, and of stars crossing the Hertzsprung gap, is characterized by the appearance of a substantial entropy gradient near the boundary of the hydrogen-depleted core. The beginnings of this jump are visible in Figure 1. The depleted core falls in specific entropy, while the deeper portion of the radiative envelope increases in entropy. It is not altogether clear what net effect these changes in thermal structure have on the dynamical stability of such stars in binary systems: the decrease in core entropy tends to be a stabilizing effect (at least for stars which have been stripped down to the enhanced entropy gradient outside the core), whereas the flattening of the entropy gradient in the envelope is ultimately destabilizing (witness the much greater tendency toward instability among stars with deep convective envelopes). Nevertheless, we suspect that, at least near the main sequence (especially the upper main sequence), nuclear evolution is a stabilizing effect. This is suggested as well by the failure of several detailed evolutionary calculations to encounter dynamical instability among late main-sequence stars (e.g., Refsdal and Weigert 1969) or post–main-sequence stars (e.g. Giannone and Giannuzzi 1972), despite their relatively extreme mass ratios ($q_i = 2.57$, or $q_i = 2.50$–3.67, respectively). The establishment of dynamical stability criteria appropriate in this regime will require more realistic models than those considered here, but a limiting mass ratio undoubtedly exists and may well be small enough to drive a significant fraction of systems transferring mass in the Hertzsprung gap into dynamical mass transfer and common envelope evolution. The result could be to increase the number of possible progenitors of cataclysmic variables and other compact binaries (see Paczyński 1976; Meyer and Meyer-Hofmeister 1979).

Condensed polytrope models are applicable to giant-branch stars, provided that their luminosities are much smaller than the Eddington limit appropriate to their core masses. The models support the general wisdom that these stars tend to expand in response to mass loss, provided that the fractional core mass is not too large ($m_c < 0.2139$). To the extent that red giants satisfying this condition have equilibrium radii which are functions only of their core masses, implying that $\zeta_{th} = 0$ (see Refsdal and Weigert 1969; Webbink, Rappaport, and Savonije 1983), they become unstable to mass transfer only on a dynamical time scale, like lower main-sequence stars, and not on a thermal time scale. For somewhat larger fractional core masses, thermal, and not dynamical time scale mass transfer occurs for a small range of mass ratios, but it is not until $m_c > 0.4567$ that systems of unit mass ratio become stable against dynamical time scale mass transfer. Since, to the extent that mass loss in a stellar wind can be neglected, the more massive star always fills its Roche lobe first (i.e., $q_i > 1$), only systems with very large fractional core masses—those with very luminous giants and large orbital separations—have the possibility of avoiding dynamical time scale mass transfer (and, presumably, common envelope evolution). This conclusion is consistent with Webbink's (1986) deductions regarding the nature of mass transfer in the progenitors of Algol binaries, symbiotic binaries with degenerate hot components, and Ba II stars. It should be pointed out, however, that the neglected roles of radiation pressure and superadiabatic convection probably render these long-period binaries more unstable than simple condensed polytropes admit.

It is important to recognize the limitations of the polytropic models used here, and more generally, of the neglect of thermal relaxation inherent in an adiabatic description of a star's adjustments to mass loss. Polytropes are merely self-gravitating spheres with a simplified equation of state. No energy sources, or energy transport, are included in the statement of the problem. Thus the response of polytropes to variations in mass is strictly that of hydrostatic readjustment. In the limit of no change in energy production and transport, or where these processes occur on a slower time scale, the polytropes can be good approximations to actual stars. However, to the extent that thermal relaxation succeeds in reestablishing a stable entropy profile in the outer envelope of a star losing mass, the onset of dynamical instability may be postponed (or even avoided) beyond the critical point indicated by the adiabatic models. Nevertheless, experience suggests that for systems near the threshold of dynamical instability, heat transport effects are small (recall Fig. 1).

VI. CONCLUSIONS

We have explored here the adiabatic responses of simple and compound polytropic models of stars to mass loss. These responses in turn establish approximate criteria for the stability or instability against dynamical time scale mass transfer of binary systems in which the donor stars are reasonably well approximated by polytropic models.

Our principal conclusions are as follows:

1. As first shown by Paczyński (1965), stars in thermal equilibrium with isentropic (convective) surface layers are linearly unstable if the mass ratio exceeds a finite critical threshold, q_0. Unless the mass fraction in these surface layers is quite small, q_0 is of the order of unity. On the other hand, stars in thermal equilibrium with subadiabatic (radiative) surface layers are linearly stable for any value of the mass ratio (N.B. Degenerate stars, although radiatively stable, may be considered effectively isentropic [with zero entropy], and therefore behave as convective stars.)

2. There exists a finite-amplitude instability to which radiative stars are subject. If the initial phases of mass transfer are sufficiently rapid (i.e. thermal time scale or faster), such a star may undergo a delayed transition to dynamical time scale mass loss. This transition is connected with the flattening of the entropy gradient in the envelope of a star as its outer layers are stripped away. For homogeneous main-sequence stars ($n = 3$, $\gamma = 5/3$), we estimate the critical mass ratio for this type of evolution to be $q_1 = 2.14$.

3. Red giants with small core mass fractions behave very much like fully convective stars, expanding adiabatically as they lose mass. As shown by Paczyński and Sienkiewicz (1972), this behavior is moderated for larger core mass fractions, so that for $m_c > 0.214$ contraction replaces expansion. For $m_c > 0.458$ (subject to the complications of large radiation pressure), it may be possible for a lobe-filling giant in a binary of unit mass ratio to remain stable against dynamical time scale mass transfer.

TABLE 4

Quantity	Units	HW	HA	RVJ
Equilibrium Complete Polytropes				
Mass	$4\pi\left(\frac{K}{4\pi G}\right)^{3/2}\rho_c^{(3-n)/2n}$	$16\sqrt{3}x^3$	$(n+1)^{3/2}\xi$	$(n+1)^{3/2}\left(-\xi^2\frac{d\theta}{d\xi}\right)$
Radius	$\left(\frac{K}{4\pi G}\right)^{1/2}\rho_c^{(1-n)/2n}$	$4\sqrt{3}\left(\frac{x^5}{-d\theta/dx}\right)^{1/4}$	$(n+1)^{1/2}f$	$(n+1)^{1/2}\xi$
Pressure	$K\rho_c^{(n+1)/n}$	θ	θ^{n+1}	θ^{n+1}
Density	ρ_c	$\theta^{n/(n+1)}$	θ^n	θ^n
Equilibrium Composite Polytropes[a]				
Mass	$4\pi\left(\frac{K_c}{4\pi G}\right)^{3/2}\rho_c^{(3-n_c)/2n_c}$	$16\sqrt{3}x_e^3$	...	$(n_e+1)^{3/2}\theta_i^{(3-n_c)/2}\left(-\xi_e^2\frac{d\theta_e}{d\xi}\right)$
Radius	$\left(\frac{K_c}{4\pi G}\right)^{1/2}\rho_c^{(1-n_c)/2n_c}$	$4\sqrt{3}\theta_i^{(\lambda-1)/4}\left(\frac{x_e^5}{-d\theta_e/dx}\right)^{1/4}$	...	$(n_e+1)^{1/2}\theta_i^{(1-n_c)/2}\xi_e$
Pressure	$K_c\rho_c^{(n_c+1)/n_c}$	$\theta_i^{1-\lambda}\theta_e$	...	$\theta_i^{n_c+1}\theta_e^{n_e+1}$
Density	ρ_c	$\theta_i^{3(n_e-n_c)/[(n_e-3)(n_c+1)]}\theta_e^{n_e/(n_e+1)}$	...	$\theta_i^{n_c}\theta_e^{n_e}$
Perturbed Complete Polytropes[b]				
Mass	$4\pi\left(\frac{K}{4\pi G}\right)^{3/2}\rho_c^{(3-n)/2n}$	$16\sqrt{3}x^3$	$(n+1)^{3/2}\xi$	...
Radius	$\left(\frac{K}{4\pi G}\right)^{1/2}\rho_c^{(1-n)/2n}$	$4\sqrt{3}\left[\frac{x^5}{-d(\omega\theta)/dx}\right]^{1/4}$	$(n+1)^{1/2}(f+g)$	...
Pressure	$K\rho_c^{(n+1)/n}$	$\omega\theta$	$(1+u)^\gamma\theta^{n+1}$	...
Density	ρ_c	$\omega^{1/\gamma}\theta^{n/(n+1)}$	$(1+u)\theta^n$	...

[a] Envelope solutions; parameters describing core solutions are identical to those in the previous table. Subscripts c refer to central values, e to envelope parameters, and i to the core solution at the core-envelope interface. The parameter λ is defined by eq. (27) of the text.

[b] Here ρ_c is the central density of the equilibrium polytrope.

There remain many circumstances in which polytropic models serve as poor approximations. For these, studies of detailed stellar models will be required to establish thresholds for dynamical time scale mass transfer. Models incorporating energy generation and heat transport are required, in any case, to establish thresholds for thermal time scale mass transfer. These will be the object of future studies.

We would like to acknowledge the support of the Research Board and the VAX Image Processing System at the University of Illinois. One of us (M. S. H.) would like to thank Dr. R. M. Hjellming for the grant of a Compaq PC upon which preliminary calculations were run. This work was supported, in part, by the National Science Foundation through grant AST 83-17916.

APPENDIX

As an aid to the reader, Table 4 gives equivalent expressions for the basic polytropic structure parameters in the formalism adopted in this paper (HW), that of Heisler and Alcock (1986; HA), and that of Rappaport, Verbunt, and Joss (1983; RVJ), which follows from Chandrasekhar (1939). Except for the introduction of a uniform system for subscripting variables, the notation is that employed by the respective papers.

REFERENCES

Acton, F. S. 1970, *Numerical Methods That Work* (New York: Harper & Row).
Benson, R. S. 1970, Ph.D. thesis, University of California, Berkeley.
British Association for the Advancement of Science. 1932, *Mathematical Tables*, Vol. 2 (London: Brit. Ass. Adv. Sci.).
Chandrasekhar, S. 1939, *An Introduction to the Study of Stellar Structure* (Chicago: University of Chicago Press).
Eggleton, P. P. 1983, *Ap. J.*, **268**, 368.
Fujimoto, M. Y. 1982*a*, *Ap. J.*, **257**, 752.
———. 1982*b*, *Ap. J.*, **257**, 767.
Giannone, P., and Giannuzzi, M. A. 1972, *Astr. Ap.*, **19**, 298.
Härm, R., and Schwarzschild, M. 1955, *Ap. J. Suppl.*, **1**, 319.
Heisler, J., and Alcock, C. 1986, *Ap. J.*, **306**, 166.
Iben, I., Jr. 1982, *Ap. J.*, **259**, 244.
Meyer, F., and Meyer-Hofmeister, E. 1979, *Astr. Ap.*, **78**, 167.
Osterbrock, D. E. 1953, *Ap. J.*, **118**, 529.
Paczyński, B. 1965, *Acta Astr.*, **15**, 89.
———. 1976, in *IAU Symposium 73, Structure and Evolution of Close Binary Systems*, ed. P. Eggleton, S. Mitton, and J. Whelan (Dordrecht: Reidel), p. 75.
Paczyński, B., and Sienkiewicz, R. 1972, *Acta Astr.*, **22**, 73.
Paczyński, B., Ziółkowski, J., and Żytkow, A. 1969, in *Mass Loss from Stars*, ed. M. Hack (Dordrecht: Reidel), p. 237.
Paczyński, B., and Żytkow, A. 1978, *Ap. J.*, **222**, 604.
Plavec, M., Ulrich, R. K., and Polidan, R. S. 1973, *Pub. A.S.P.*, **85**, 769.
Rappaport, S. A., Joss, P. C., and Webbink, R. F. 1982, *Ap. J.*, **254**, 616.
Rappaport, S. A., Verbunt, F., and Joss, P. C. 1983, *Ap. J.*, **275**, 713.
Refsdal, S., and Weigert, A. 1969, *Astr. Ap.*, **1**, 167.
Ritter, H. 1976, *M.N.R.A.S.*, **175**, 279.
Schwarzschild, M. 1958, *Structure and Evolution of the Stars* (New York: Dover).
Service, A. T. 1977, *Ap. J.*, **211**, 908.
Tutukov, A. V., Fedorova, A. V., and Yungel'son, L. R. 1982, *Pis'ma Astr. Zh.*, **8**, 365 (English transl., in *Soviet Astr. Letters*, **8**, 198 [1983]).
Webbink, R. F. 1976, *Ap. J. Suppl.*, **32**, 583.
———. 1977, *Ap. J.*, **211**, 486.
———. 1985, in *Interacting Binary Stars*, ed. J. E. Pringle and R. A. Wade (Cambridge: Cambridge University Press), p. 39.
———. 1986, in *Critical Observations versus Physical Models for Close Binary Systems*, ed. K.-C. Leung and D.-S. Zhai (New York: Gordon & Breach), in press.
Webbink, R. F., Rappaport, S. A., and Savonije, G. J. 1983, *Ap. J.*, **270**, 678.
Yungel'son, L. R. 1973, *Nauch. Inf.*, **27**, 93.

MICHAEL S. HJELLMING and RONALD F. WEBBINK: Department of Astronomy, University of Illinois, 1011 W. Springfield, Urbana, IL 61801